

# pFedAFM: Adaptive Feature Mixture for Batch-Level Personalization in Heterogeneous Federated Learning

Liping Yi

yiliping@nbjl.nankai.edu.cn  
College of Computer Science, TMCC,  
SysNet, DISec, GTIISC,  
Nankai University  
Tianjin, China

Han Yu

han.yu@ntu.edu.sg  
College of Computing and Data  
Science, Nanyang Technological  
University (NTU)  
Singapore

Chao Ren

chao.ren@ntu.edu.sg  
College of Computing and Data  
Science, Nanyang Technological  
University (NTU)  
Singapore

Heng Zhang

hengzhang@tju.edu.cn  
College of Intelligence and  
Computing, Tianjin University  
Tianjin, China

Gang Wang

wgzwp@nbjl.nankai.edu.cn  
College of Computer Science, TMCC,  
SysNet, DISec, GTIISC,  
Nankai University  
Tianjin, China

Xiaoguang Liu

liuxg@nbjl.nankai.edu.cn  
College of Computer Science, TMCC,  
SysNet, DISec, GTIISC,  
Nankai University  
Tianjin, China

Xiaoxiao Li

xiaoxiao.li@ece.ubc.ca  
Department of Electrical and  
Computer Engineering,  
The University of British Columbia  
Vancouver, BC, Canada

## ABSTRACT

Model-heterogeneous personalized federated learning (MHPFL) enables FL clients to train structurally different personalized models on non-independent and identically distributed (non-IID) local data. Existing MHPFL methods focus on achieving client-level personalization, but cannot address batch-level data heterogeneity. To bridge this important gap, we propose a model-heterogeneous personalized Federated learning approach with Adaptive Feature Mixture (pFedAFM) for supervised learning tasks. It consists of three novel designs: 1) A sharing global homogeneous small feature extractor is assigned alongside each client’s local heterogeneous model (consisting of a heterogeneous feature extractor and a prediction header) to facilitate cross-client knowledge fusion. The two feature extractors share the local heterogeneous model’s prediction header containing rich personalized prediction knowledge to retain personalized prediction capabilities. 2) An iterative training strategy is designed to alternately train the global homogeneous small feature extractor and the local heterogeneous large model for effective global-local knowledge exchange. 3) A trainable weight vector is designed to dynamically mix the features extracted by both feature extractors to adapt to batch-level data heterogeneity. Theoretical analysis proves that pFedAFM can converge over time. Extensive experiments on 2 benchmark datasets demonstrate that it significantly outperforms 7 state-of-the-art MHPFL methods, achieving up to 7.93% accuracy improvement while incurring low communication and computation costs.

## KEYWORDS

Personalized Federated Learning, Model Heterogeneity, Data Heterogeneity, System Heterogeneity, Adaptive Feature Mixture

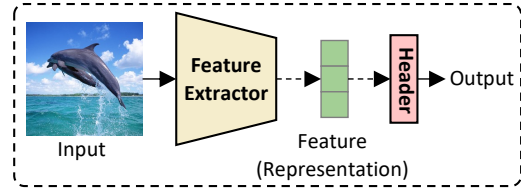


Figure 1: Feature extractor and prediction header.

## 1 INTRODUCTION

Federated learning (FL) [19] is a distributed collaborative machine learning paradigm. It typically leverages an FL server to coordinate multiple FL clients to train a shared global model without exposing potentially sensitive local data, thereby preserving data privacy [39, 46, 53].

Clients participating in FL are often devices with diverse system configurations in terms of communication bandwidth, computing power, memory and storage (*a.k.a.*, system heterogeneity) [45, 47]. They can also possess non-IID data (*a.k.a.*, data heterogeneity) due to differences in usage environments [43, 44]. Classical FL aggregation approaches, such as FedAvg [28], require the server to broadcast the global model to the clients for training on local data. The trained local models are then sent back to the server for aggregation. Thus, all clients are required to train models of the same structure. This forces all clients to train a homogeneous model with a size that can be supported by the most resource-constrained client device, thereby limiting global model performance and wasting the system resources of higher-end client devices. Besides, a single global model for all clients often cannot perform well on each client’s non-IID

local data [60]. Furthermore, clients with proprietary models might be reluctant to share their model structures with others due to intellectual property protection concerns [48, 50]. In response to these challenges, the field of Model-Heterogeneous Personalized Federated Learning (MHPFL) [49, 51, 52] has emerged to enable clients to train local models with diverse structures, while still joining FL.

Existing MHPFL methods take one of the following two main approaches: (1) The server or clients pruning the global model into subnets with different structures and aggregating them by parameter positions, constraining the relationship between the global model and client models [11, 13]; and (2) clients training structurally unrelated local models, supporting higher levels of model heterogeneity [48]. Our research focuses on the second approach due to its practicality. It leverages three main techniques: knowledge distillation, model mixture and mutual learning. Knowledge distillation-based MHPFL methods [15, 21] often rely on the availability of a suitable public dataset. This is hard to achieve in practice. Model mixture-based MHPFL methods [10, 23] share the homogeneous parts of heterogeneous local models for FL aggregation. They often face model performance bottlenecks and exposure to partial model structures (which can compromise privacy). Mutual learning-based MHPFL methods [33, 42] equip each client’s heterogeneous local model with an additional small homogeneous model. The two models exchange local and global knowledge via mutual learning. The small homogeneous local models are used for FL aggregation at the server. However, model performance improvements tend to be small due to the limitations of mutual learning.

Existing MHPFL methods are designed for client-level personalization. They cannot deal with the problem of data distribution variations across local training batches (*i.e.*, *batch-level data heterogeneity*), which often take place. To bridge this important gap, we propose the model-heterogeneous personalized Federated learning approach with Adaptive Feature Mixture (pFedAFM) for supervised learning tasks. It consists of three novel designs: **(1) Model Architecture**: We split each client’s local heterogeneous model into two parts: 1) a heterogeneous feature extractor, and 2) a prediction header as in Figure 1. A shared global small homogeneous feature extractor is additionally assigned to each client for cross-client knowledge sharing. The two feature extractors share the same prediction header. **(2) Model Training**: We design an iterative training method to train the two models alternatively for bidirectionally transferring the global generalized and local personalized knowledge between the server and clients. **(3) Adaptive Feature Mixing**: For each training batch, each client trains a personalized trainable weight vector to mix the representations extracted by the two feature extractors. The weighted mixed representations are processed by the header for prediction. Then, the trainable weight vector and the local heterogeneous model are updated simultaneously. In this way, pFedAFM achieves batch-level personalization through fine-grained representation mixing in response to local data distribution variations across different training batches.

Theoretical analysis proves that it converges over time with a  $\mathcal{O}(1/T)$  non-convex convergence rate. Experiments on 2 benchmark datasets across 7 state-of-the-art MHPFL methods demonstrate its

superiority in model performance, achieving up to 7.93% accuracy improvement with low communication and computation costs.

## 2 RELATED WORK

MHPFL works can be classified into two families: (1) Clients training heterogeneous subnets of the global model: these local heterogeneous subnets are aggregated at the server by parameter ordinates. These methods (*e.g.*, FedRoLex [3], FLASH [4], InCo [5], HeteroFL [11], FjORD [13], HFL [26], Fed2 [54], FedResCuE [62]) often utilize model pruning techniques to construct heterogeneous subnets, incurring high computational overheads and limiting the relationships between client models. (2) Clients training heterogeneous models with diverse structures: it offers high flexibility in model heterogeneity. Our work falls under the latter family, which can be further divided into three types based on the techniques adopted.

**MHPFL with Knowledge Distillation.** Most of these methods (Cronus [6], FedGEMS [8], Fed-ET [9], FSFL [14], FCCL [15], DS-FL [16], FedMD [21], FedKT [22], FedDF [24], FedHeNN [27], FedKEM [29], KRR-KD [31], FedAUX [35], CFD [36], pFedHR [41], FedKEMF [55] and KT-pFL [56]) rely on an additional labeled or unlabelled public data with a similar distribution to the client’s local data, which is not often accessible in practice due to data privacy concerns. Communication and computational overhead involving all samples of the public dataset is high. To avoid using an extra public dataset, some methods (*e.g.*, FedGD [57], FedZKT [58], FedGen [61]) train a generator to generate synthetic public data, which introduces high training costs. Remaining methods (*e.g.*, HFD [1, 2], FedGKT [12], FD [18], FedProto [40], and FedGH [48]) aggregate seen-class information from clients by class at the server, which risks privacy leakage due to uploading class information.

**MHPFL with Model Mixture.** These methods divide a client’s local model as two parts: a feature extractor and a prediction header. Different clients may possess heterogeneous feature extractors and homogeneous prediction headers, with the latter being shared for aggregation (*e.g.*, FedMatch [7], FedRep [10], FedBABU [30] and FedAlt/FedSim [32]). In contrast, other methods (FedClassAvg [17], LG-FedAvg [23] and CHFL [25]) share the homogeneous feature extractors, while keeping heterogeneous prediction header private. Sharing parts of the local models leaks partial model structure and leads to performance bottlenecks.

**MHPFL with Mutual Learning.** These methods (FML [38] and FedKD [42]) add a small homogeneous model to each client’s local heterogeneous model. Clients train them through mutual learning, and the server aggregates the locally trained small homogeneous models. However, the improperly trained shared small homogeneous model during early rounds of FL might negatively affect model convergence. To solve this issue, a recent MHPFL research - FedAPEN [33], based on mutual learning, allows each client to first train a personalized learnable weight on partial local data for the output logits of the local heterogeneous model. Then, it performs 1- operation on this weight as the weight of the homogeneous small model’s output logits. Fixing the two weights, it then trains these models via end-to-end mutual learning on the remaining local data. It achieves client-level personalization by training a learnable weight for the output ensemble. However, the fixed weight during model training might negatively impact model performance

due to the distribution divergences between the partial data for training the learnable weight versus the remaining data. This can be further exacerbated by the batch-level data heterogeneity issue. Moreover, different dimensions of the model output logits contain different semantic information. Sharing the same weight for all output dimensions fails to exploit the differences in the importance of semantic information across different dimensions, thereby limiting model performance.

Existing MHPFL methods are not designed to deal with the issue of batch-level data heterogeneity. To the best of our knowledge, pFedAFM is the first approach to bridge this important gap by fine-grained dimension-level representation mixing adaptive to local data distribution variations across different training batches.

### 3 PROBLEM FORMULATION

Under pFedAFM, a central FL server coordinates  $N$  FL clients with heterogeneous local models for collaborative training. In each communication round, a fraction  $C$  of the  $N$  clients join FL model training. The selected client set is denoted as  $\mathcal{S}$ ,  $|\mathcal{S}| = C \cdot N = K$ . The local heterogeneous model  $\mathcal{F}_k(\omega_k)$  held by client  $k$  ( $\mathcal{F}_k(\cdot)$  is the heterogeneous model structure,  $\omega_k$  are the personalized model parameters) consists of a feature extractor  $\mathcal{F}_k^{ex}(\omega_k^{ex})$  and a prediction header  $\mathcal{F}_k^{hd}(\omega_k^{hd})$ . Client  $k$ 's non-IID local dataset  $D_k$  follows distribution  $P_k$ . To achieve knowledge sharing across heterogeneous clients, a small homogeneous global shared feature extractor  $\mathcal{G}(\theta)$  ( $\mathcal{G}(\cdot)$  is the homogeneous model structure,  $\theta$  are parameters) is assigned to each client. After training the two models locally via the proposed iterative training method,  $\mathcal{G}(\theta_k)$  is uploaded to the server for aggregation. Therefore, the training objective of pFedAFM is to minimize the sum of the loss of the combined complete model  $\mathcal{H}_k(h_k) = \mathcal{G}(\theta) \circ \mathcal{F}_k(\omega_k)$  of all clients on local data  $D_k$ :

$$\min_{\theta, \omega_0, \dots, \omega_{N-1}} \sum_{k=0}^{N-1} \ell(\mathcal{H}_k(D_k; \theta \circ \omega_k)). \quad (1)$$

### 4 THE PROPOSED APPROACH

pFedAFM consists of three key design considerations as follows.

**(1) Model Architecture.** We cannot directly aggregate local models with heterogeneous structures at the server. Since the representations extracted by the feature extractor contain richer semantic information than model output logits and the local heterogeneous model's header closer to model output carries sufficient personalized prediction information, we additionally assign a global shared homogeneous small feature extractor to all clients, and the homogeneous small feature extractor and the local heterogeneous model's feature extractor shares the local heterogeneous model's prediction header. The locally updated homogeneous small feature extractors are aggregated at the server for cross-client knowledge fusion.

**(2) Model Training.** An intuitive way to train the homogeneous small feature extractor and the local heterogeneous model is updating them simultaneously in an end-to-end manner. However, the immature global homogeneous feature extractor in early rounds may harm model performance within end-to-end training, and the complete global information is only transferred to clients within the first local iteration. To address these concerns, we devise an iterative training approach. Firstly, we freeze the global shared

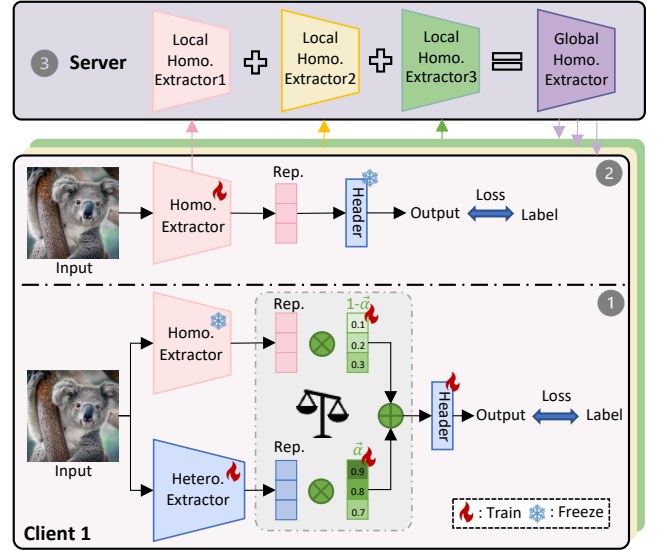


Figure 2: Workflow of pFedAFM.

homogeneous small feature extractor, and train the local heterogeneous model's feature extractor and prediction header, transferring knowledge from global to local. Then, we freeze the local heterogeneous model's prediction header and train the global homogeneous small feature extractor, transferring knowledge from local to global.

**(3) Adaptive Feature Mixing.** In the first step of iterative training, we train a pair of trainable weight vectors for weighting the representations extracted by the global homogeneous small feature extractor and the local heterogeneous feature extractor. Each dimension of the weight vector corresponds to a dimension of the representation, achieving a finer-grained feature mixture. The weighted mixed representations absorb the generalized feature information from the global homogeneous small feature extractor and the personalized feature information from the local heterogeneous feature extractor. Moreover, the trainable weight vector is updated simultaneously with the local heterogeneous model, which dynamically balances the generalization and personalization of local models adaptive to the distribution variations across different batches, *i.e.*, achieving adaptive batch-level personalization.

**Overview.** With the above considerations, we design pFedAFM to perform the following steps in each training round (Figure 2).

- ① Each client receives the global homogeneous small feature extractor from the server and freezes its parameters to train the local heterogeneous model feature extractor and prediction header. In a training batch, a pair of trainable weight vectors weigh the representations extracted by the two feature extractors on local data samples of this batch to produce the mixed representations, which are further processed by the local heterogeneous model's prediction header to output predictions. The loss between the predictions and the labels is used to update the parameters of the local heterogeneous model and the trainable weight vectors.
- ② Each client freezes the updated parameters of the local heterogeneous model's prediction header and feeds local data

samples into the global homogeneous feature extractor to extract representations. They are further fed into the frozen prediction header to produce predictions. The loss between the predictions and the labels is used to update the parameters of the homogeneous small feature extractor.

- ③ The updated local homogeneous small feature extractor is uploaded to the server for aggregation to produce the new global homogeneous feature extractor. It is then distributed to clients participating in the next round of FL.

The three steps repeat until all clients' local combined heterogeneous models (the mixture of the local heterogeneous model and the global homogeneous small feature extractor) converge, which is used to perform inference after FL training. The details of pFedAFM are given in Algorithm 1.

## 4.1 Knowledge Exchange by Iterative Training

**4.1.1 Local Heterogeneous Model Training with Adaptive Batch-Level Personalization.** In the  $t$ -th communication round, for global-to-local knowledge transfer, a client  $k$  freezes the received global homogeneous small feature extractor  $\mathcal{G}(\theta^{t-1})$ , and trains its local heterogeneous model's feature extractor  $\mathcal{F}_k^{ex}(\omega_k^{ex,t-1})$  and prediction header  $\mathcal{F}_k^{hd}(\omega_k^{hd,t-1})$ . Specifically, for each data sample  $(x_i, y_i) \in D_k$ ,  $x_i$  is fed into the frozen  $\mathcal{G}(\theta^{t-1})$ , which contains generalized feature information across all labels, to extract generalized representations. It is also fed into  $\mathcal{F}_k^{ex}(\omega_k^{ex,t-1})$ , which contains local personalized feature information across seen classes, to extract personalized representations.

$$\mathcal{R}_i^{\mathcal{G}} = \mathcal{G}(x_i; \theta^{t-1}), \mathcal{R}_i^{\mathcal{F}_k} = \mathcal{F}_k^{ex}(x_i; \omega_k^{ex,t-1}). \quad (2)$$

To effectively balance the generalization and personalization of local models, we learn a trainable weight vector  $\alpha_{k,i}^{t-1}$  to weigh the representations  $\mathcal{R}_i^{\mathcal{F}_k}$  extracted by the local heterogeneous feature extractor.  $1 - \alpha_{k,i}^{t-1}$  is the weight vector for weighing the representations  $\mathcal{R}_i^{\mathcal{G}}$  extracted by the frozen global homogeneous small feature extractor. The two weight vectors have the same dimensions as the representations. The representations extracted by two feature extractors are dot-multiplied with their corresponding weight vectors, then summed element-wise to produce the mixed representations:

$$\mathcal{R}_i = \mathcal{R}_i^{\mathcal{G}} \cdot (1 - \alpha_{k,i}^{t-1}) + \mathcal{R}_i^{\mathcal{F}_k} \cdot \alpha_{k,i}^{t-1}. \quad (3)$$

Mixing the representations extracted by two feature extractors via weighted summation requires the dimension of the last linear layer of the two feature extractors to be the same. For a client with a structure-agnostic local model (*i.e.*, black box), if its penultimate layer is linear (*i.e.*, the last linear layer is the prediction header), it needs to modify the penultimate layer dimension to be the same as the last linear layer dimension of the global homogeneous feature extractor. If its penultimate layer is non-linear, it needs to add a linear layer with an identical dimension to the global homogeneous feature extractor's last linear layer ahead of the prediction header. This dimension-matching step is straightforward to implement.

The mixed representation  $\mathcal{R}_i$  fuses global generalized and local personalized feature information. The mixed representation  $\mathcal{R}_i$  is then fed into the local heterogeneous model's prediction header

### Algorithm 1: pFedAFM

**Input:**  $N$ , total number of clients;  $K$ , number of selected clients in one round;  $T$ , number of communication rounds;  $\eta_\omega$ , learning rate of local heterogeneous models;  $\eta_\alpha$ , learning rate of trainable weight vector;  $\eta_\theta$ , learning rate of homogeneous feature extractor.

Randomly initialize global homogeneous feature extractor  $\mathcal{G}(\theta^0)$ , local trainable weight vectors  $[\alpha_0, \dots, \alpha_{N-1}] = \mathbf{1}$ , and local heterogeneous models  $[\mathcal{F}_0(\omega_0^0), \dots, \mathcal{F}_{N-1}(\omega_{N-1}^0)]$ .

**for**  $t = 1$  **to**  $T - 1$  **do**

**// Server Side:**

$\mathcal{S}^t \leftarrow$  Randomly select  $K \leq N$  clients to join FL;

    Broadcast the global homogeneous feature extractor

$\theta^{t-1}$  to selected  $K$  clients;

$\theta_k^t \leftarrow$  **ClientUpdate**( $\theta^{t-1}$ );

**/\* Aggregate Homogeneous Feature Extractors \*/**

$\theta^t = \sum_{k \in \mathcal{S}^t} \frac{n_k}{n} \theta_k^t$ .

**// ClientUpdate:**

    Receive the global homogeneous feature extractor  $\theta^{t-1}$  from the server;

**for**  $k \in \mathcal{S}^t$  **do**

**/\* Freeze Homo. Extractor, Train Hetero. Model \*/**

**for**  $(x_i, y_i) \in D_k$  **do**

$\mathcal{R}_i^{\mathcal{G}} = \mathcal{G}(x_i; \theta^{t-1}), \mathcal{R}_i^{\mathcal{F}_k} = \mathcal{F}_k^{ex}(x_i; \omega_k^{ex,t-1});$

$\mathcal{R}_i = \mathcal{R}_i^{\mathcal{G}} \cdot (1 - \alpha_{k,i}^{t-1}) + \mathcal{R}_i^{\mathcal{F}_k} \cdot \alpha_{k,i}^{t-1};$

$\hat{y}_i = \mathcal{F}_k^{hd}(\mathcal{R}_i; \omega_k^{hd,t-1});$

$\ell_i = \ell(\hat{y}_i, y_i);$

$\omega_k^t \leftarrow \omega_k^{t-1} - \eta_\omega \nabla \ell_i;$

$\alpha_{k,i}^t \leftarrow \alpha_{k,i}^{t-1} - \eta_\alpha \nabla \ell_i;$

**end**

**/\* Freeze Hetero. Model, Train Homo. Extractor \*/**

**for**  $(x_i, y_i) \in D_k$  **do**

$\mathcal{R}_i = \mathcal{G}(x_i; \theta^{t-1});$

$\hat{y}_i = \mathcal{F}_k^{hd}(\mathcal{R}_i; \omega_k^{hd,t-1});$

$\ell_i = \ell(\hat{y}_i, y_i);$

$\theta^t \leftarrow \theta^{t-1} - \eta_\theta \nabla \ell_i;$

**end**

    Upload trained local homogeneous feature extractor  $\theta_k^t$  to the server.

**end**

**end**

**Output:** heterogeneous local complete mixed models

$[(\mathcal{G}(\theta^{T-1}) \circ \mathcal{F}_0(\omega_0^{T-1}) | \alpha_0^{T-1}), \dots, (\mathcal{G}(\theta^{T-1}) \circ \mathcal{F}_{N-1}(\omega_{N-1}^{T-1}) | \alpha_{N-1}^{T-1})]$ .

$\mathcal{F}_k^{hd}(\omega_k^{hd,t-1})$  to produce predictions:

$$\hat{y}_i = \mathcal{F}_k^{hd}(\mathcal{R}_i; \omega_k^{hd,t-1}). \quad (4)$$

Then, the loss (*e.g.*, cross-entropy loss [59] in classification tasks) between prediction  $\hat{y}_i$  and label  $y_i$  is computed as:

$$\ell_i = \ell(\hat{y}_i, y_i). \quad (5)$$

The loss is used to update the parameters of the local heterogeneous model and the pair of trainable weight vectors via gradient descent (e.g., SGD optimizer [34]):

$$\begin{aligned}\omega_k^t &\leftarrow \omega_k^{t-1} - \eta_\omega \nabla \ell_i, \\ \alpha_{k,i}^t &\leftarrow \alpha_{k,i}^{t-1} - \eta_\alpha \nabla \ell_i,\end{aligned}\quad (6)$$

where  $\eta_\omega$  and  $\eta_\alpha$  are the learning rates of the local heterogeneous model and the trainable weight vectors. Therefore, the trainable weight vectors dynamically balance the generalization and personalization as the data distribution varies across different training batches, thereby achieving adaptive batch-level personalization.

**4.1.2 Global Homogeneous Feature Extractor Training.** After training the local heterogeneous model, a client  $k$  freezes its local header  $\mathcal{F}_k^{hd}(\omega_k^{hd,t})$  and trains the global homogeneous small feature extractor on local data  $D_k$  for local-to-global knowledge transfer.

Specifically, client  $k$  inputs each sample  $(x_i, y_i) \in D_k$  into the global homogeneous feature extractor to extract its representation:

$$\mathcal{R}_i = \mathcal{G}(x_i; \theta^{t-1}). \quad (7)$$

The representation is then fed into the frozen local heterogeneous model's prediction header  $\mathcal{F}_k^{hd}(\omega_k^{hd,t})$  to produce a prediction:

$$\hat{y}_i = \mathcal{F}_k^{hd}(\mathcal{R}_i; \omega_k^{hd,t}). \quad (8)$$

The loss between the prediction and the label is then computed as:

$$\ell_i = \ell(\hat{y}_i, y_i). \quad (9)$$

The homogeneous feature extractor is updated via gradient descent:

$$\theta^t \leftarrow \theta^{t-1} - \eta_\theta \nabla \ell_i, \quad (10)$$

where  $\eta_\theta$  is the learning rate of the homogeneous feature extractor. We set  $\eta_\theta = \eta_\omega$  to ensure stable convergence of local models.

## 4.2 Knowledge Fusion across Clients

Client  $k$  sends its updated local homogeneous extractor  $\theta_k^t$  to the server for aggregation to fuse cross-client knowledge:

$$\theta^t = \sum_{k \in \mathcal{S}^t} \frac{n_k}{n} \theta_k^t, \quad (11)$$

where  $n_k = |D_k|$  is the size of client  $k$ 's local dataset  $D_k$ , and  $n$  is the total size of all clients' local datasets.

**Summary.** We view local homogeneous small feature extractors as the carriers of local knowledge and enable knowledge fusion across heterogeneous local models by sharing them. Through iterative training of the global shared small homogeneous feature extractor and local heterogeneous models, we achieve effective bidirectional knowledge transfer. Through dimension-wise mixing of generalized features and personalized features, pFedAFM adaptively balances model generalization and personalization at the batch level. Hence, the objective of pFedAFM in Eq. (1) can be refined as:

$$\min_{\theta, \omega_0, \dots, \omega_{N-1}} \sum_{k=0}^{N-1} \ell(\mathcal{F}_k(D_k; \theta \cdot (1 - \alpha_k) + \omega_k \cdot \alpha_k)). \quad (12)$$

## 5 CONVERGENCE ANALYSIS

We clarify some notations.  $t \in \{0, \dots, T-1\}$  is the  $t$ -th communication round.  $e \in \{0, 1, \dots, E\}$  is the  $e$ -th local iteration.  $tE+0$  denotes the start of the  $(t+1)$ -th round in which client  $k$  in the  $(t+1)$ -th round receives the small homogeneous feature extractor  $\mathcal{G}(\theta^t)$  from the server.  $tE+e$  is the  $e$ -th local iteration in the  $(t+1)$ -th round.  $tE+E$  is the last local iteration in the  $(t+1)$ -th round. After that, client  $k$  sends its local updated small homogeneous feature extractor the server for aggregation.  $\mathcal{H}_k(h_k)$  is client  $k$ 's entire local model consisting of the global small homogeneous feature extractor  $\mathcal{G}(\theta)$  and the local heterogeneous model  $\mathcal{F}_k(\omega_k)$  weighed by the trainable weight vector  $\alpha_k$ , i.e.,  $\mathcal{H}_k(h_k) = (\mathcal{G}(\theta) \circ \mathcal{F}_k(\omega_k))\alpha_k$ .  $\eta$  is the learning rate of client  $k$ 's local model  $\mathcal{H}_k(h_k)$ , consisting of  $\{\eta_\theta, \eta_\omega, \eta_\alpha\}$ .

**ASSUMPTION 1. Lipschitz Smoothness.** The gradients of client  $k$ 's entire local heterogeneous model  $h_k$  are  $L_1$ -Lipschitz smooth [40],

$$\|\nabla \mathcal{L}_k^{t_1}(h_k^{t_1}; x, y) - \nabla \mathcal{L}_k^{t_2}(h_k^{t_2}; x, y)\| \leq L_1 \|h_k^{t_1} - h_k^{t_2}\|, \quad (13)$$

$$\forall t_1, t_2 > 0, k \in \{0, 1, \dots, N-1\}, (x, y) \in D_k.$$

The above formulation can be re-expressed as:

$$\mathcal{L}_k^{t_1} - \mathcal{L}_k^{t_2} \leq \langle \nabla \mathcal{L}_k^{t_2}, (h_k^{t_1} - h_k^{t_2}) \rangle + \frac{L_1}{2} \|h_k^{t_1} - h_k^{t_2}\|_2^2. \quad (14)$$

**ASSUMPTION 2. Unbiased Gradient and Bounded Variance.** Client  $k$ 's random gradient  $g_{h,k}^t = \nabla \mathcal{L}_k^t(h_k^t; \mathcal{B}_k^t)$  ( $\mathcal{B}$  is a batch of local data) is unbiased,

$$\mathbb{E}_{\mathcal{B}_k^t \subseteq D_k} [g_{h,k}^t] = \nabla \mathcal{L}_k^t(h_k^t), \quad (15)$$

and the variance of random gradient  $g_{h,k}^t$  is bounded by:

$$\mathbb{E}_{\mathcal{B}_k^t \subseteq D_k} [\|\nabla \mathcal{L}_k^t(h_k^t; \mathcal{B}_k^t) - \nabla \mathcal{L}_k^t(h_k^t)\|_2^2] \leq \sigma^2. \quad (16)$$

**ASSUMPTION 3. Bounded Parameter Variation.** The parameter variations of the small homogeneous feature extractor  $\theta_k^t$  and  $\theta^t$  before and after aggregation at the FL server is bounded by:

$$\|\theta^t - \theta_k^t\|_2 \leq \delta^2. \quad (17)$$

Based on the above assumptions, we can derive the following Lemma and Theorem. Detailed proofs are given in Appendix A.

**LEMMA 1. Local Training.** Given Assumptions 1 and 2, the loss of an arbitrary client's local model  $h$  in the  $(t+1)$ -th local training round is bounded by:

$$\mathbb{E}[\mathcal{L}_{(t+1)E}] \leq \mathcal{L}_{tE+0} + \left(\frac{L_1 \eta^2}{2} - \eta\right) \sum_{e=0}^E \|\nabla \mathcal{L}_{tE+e}\|_2^2 + \frac{L_1 E \eta^2 \sigma^2}{2}. \quad (18)$$

**LEMMA 2. Model Aggregation.** Given Assumptions 2 and 3, after the  $(t+1)$ -th local training round, the loss of any client before and after aggregating the small homogeneous feature extractors at the FL server is bounded by:

$$\mathbb{E}[\mathcal{L}_{(t+1)E+0}] \leq \mathbb{E}[\mathcal{L}_{tE+1}] + \eta \delta^2. \quad (19)$$

**THEOREM 1. One Complete Round of FL.** Based on Lemma 1 and Lemma 2, for any client, after local training, model aggregation and receiving the new global homogeneous feature extractor, we have:

$$\mathbb{E}[\mathcal{L}_{(t+1)E+0}] \leq \mathcal{L}_{tE+0} + \left(\frac{L_1 \eta^2}{2} - \eta\right) \sum_{e=0}^E \|\nabla \mathcal{L}_{tE+e}\|_2^2 + \frac{L_1 E \eta^2 \sigma^2}{2} + \eta \delta^2. \quad (20)$$

**THEOREM 2. Non-convex Convergence Rate of pFedAFM.** With Theorem 1, for any client and an arbitrary constant  $\epsilon > 0$ , the following holds:

$$\frac{1}{T} \sum_{t=0}^{T-1} \sum_{e=0}^{E-1} \|\nabla \mathcal{L}_{tE+e}\|_2^2 \leq \frac{\frac{1}{T} \sum_{t=0}^{T-1} [\mathcal{L}_{tE+0} - \mathbb{E}[\mathcal{L}_{(t+1)E+0}]] + \frac{L_1 E \eta^2 \sigma^2}{2} + \eta \delta^2}{\eta - \frac{L_1 \eta^2}{2}} < \epsilon, \\ \text{s.t. } \eta < \frac{2(\epsilon - \delta^2)}{L_1(\epsilon + E\sigma^2)}. \quad (21)$$

Therefore, we conclude that any client’s local model can converge at a non-convex rate of  $\epsilon \sim \mathcal{O}(1/T)$  in pFedAFM if the learning rates of the homogeneous feature extractor, local heterogeneous model and the trainable weight vector satisfy the above condition.

## 6 EXPERIMENTAL EVALUATION

We implement pFedAFM and 7 state-of-the-art MHPFL baselines with Pytorch, and evaluate performances over 2 benchmark datasets on 4 NVIDIA GeForce RTX 3090 GPUs with 24 GB memory.

### 6.1 Experiment Setup

**Datasets.** We test the performances of pFedAFM and baselines on benchmark image datasets CIFAR-10 and CIFAR-100<sup>1</sup> [20] which are commonly used by FL image classification tasks. CIFAR-10 contains 6,000 10-class colourful images with  $32 \times 32$  size, with 5,000 images for training and 1,000 images for testing. CIFAR-100 contains 100 classes of colourful images with  $32 \times 32$  size. Each class contains 500 training images and 100 testing images. We use two typical approaches to construct non-IID datasets. (1) Pathological [37]: we assign 2 classes of CIFAR-10 samples to each client, denoted as (non-IID: 2/10); and assign 10 classes of CIFAR-100 samples to each client, marked as (non-IID: 10/100). (2) Practical [33]: we assign all classes of CIFAR-10 or CIFAR-100 samples to each client and use a Dirichlet( $\gamma$ ) function to produce different counts of each class on different clients. A smaller  $\gamma$  controls a higher non-IID degree. For each client’s assigned non-IID local dataset, we further divide it into a training set and a testing set with a ratio of 8 : 2 (*i.e.*, they follow the same distribution).

**Base Models.** Model homogeneity is a special case of model heterogeneity. We test algorithms under both model-homogeneous and model-heterogeneous FL scenarios. In the model-homogeneous FL scenario, we assign the same CNN-1 (Table 1) to all clients. In model-heterogeneous FL scenario, we allocate 5 heterogeneous models {CNN-1, ..., CNN-5} (Table 1) to clients, and each client’s heterogeneous model id is determined by client id %5. For the added homogeneous small model or homogeneous feature extractor in mutual learning-based FML, FedKD, FedAPEN and pFedAFM, we choose the smallest CNN-5 or CNN-5 without the last linear layer.

**Comparison Baselines.** We compare pFedAFM with the state-of-the-art MHPFL methods belonging to the three most related heterogeneity-flexible MHPFL works outlined in Section 2.

- **Standalone.** Each client trains its local heterogeneous model only with local data (*i.e.*, no FL).
- **MHPFL via Public Data-Independent Knowledge Distillation:** FD [18] and FedProto [40].
- **MHPFL via Model Mixture:** LG-FedAvg [23].

**Table 1: Structures of 5 heterogeneous CNN models with  $5 \times 5$  kernel size and 16 or 32 filters in convolutional layers.**

| Layer Name | CNN-1    | CNN-2   | CNN-3   | CNN-4   | CNN-5   |
|------------|----------|---------|---------|---------|---------|
| Conv1      | 5×5, 16  | 5×5, 16 | 5×5, 16 | 5×5, 16 | 5×5, 16 |
| Maxpool1   | 2×2      | 2×2     | 2×2     | 2×2     | 2×2     |
| Conv2      | 5×5, 32  | 5×5, 16 | 5×5, 32 | 5×5, 32 | 5×5, 32 |
| Maxpool2   | 2×2      | 2×2     | 2×2     | 2×2     | 2×2     |
| FC1        | 2000     | 2000    | 1000    | 800     | 500     |
| FC2        | 500      | 500     | 500     | 500     | 500     |
| FC3        | 10/100   | 10/100  | 10/100  | 10/100  | 10/100  |
| model size | 10.00 MB | 6.92 MB | 5.04 MB | 3.81 MB | 2.55 MB |

- **MHPFL via Mutual Learning:** FML [38], FedKD [42], and FedAPEN [33]. Our pFedAFM also belongs to this category.

**Evaluation Metrics.** We compare the performance of MHPFL methods with the following evaluation metrics:

- **Model Accuracy.** We trace each client’s local model’s individual accuracy varied as rounds and compute each round’s mean accuracy of all participating clients. We report the highest mean accuracy among all rounds and the individual accuracy of all clients in the last round.
- **Communication Cost.** We calculate the average number of parameters communicated between clients and the server in one round and monitor the rounds required to attain the specified target mean accuracy. The product of the two is the overall communication cost.
- **Computation Overhead.** We calculate the average computational FLOPs of clients in one round and monitor the rounds required for target mean accuracy. The product of the two is the overall computational overhead.

**Training Strategy.** We use grid-search to find the optimal FL hyperparameters and specific hyperparameters for all algorithms. For FL hyperparameters, we test them with batch size = {64, 128, 256, 512}, local epochs = {1, 10}, total rounds  $T = \{100, 500\}$ , SGD optimizer with a 0.01 learning rate. In pFedAFM, we vary  $\eta_\alpha = \{0.001, 0.01, 0.1, 1\}$ . We report the highest mean accuracy for all algorithms.

### 6.2 Results and Discussion

To test the stability of MHPFL algorithms, we compare them under different client numbers  $N$  and client participation rates  $C$ :  $\{(N = 10, C = 100\%), (N = 50, C = 20\%), (N = 100, C = 10\%)\}$ .

**6.2.1 Model-Homogeneous FL.** Table 2 shows that pFedAFM reaches the highest mean accuracy across all FL settings. It improves up to 7.76% accuracy than each FL setting’s state-of-the-art baseline and increases up to 11.70% accuracy than each FL setting’s same-category (mutual learning) best baseline. This indicates that the batch-level personalization by dynamically mixing generalized and personalized features adaptive to local data distribution in pFedAFM takes a better balance between model generalization and personalization, hence promoting significant accuracy improvements.

**6.2.2 Model-Heterogeneous FL.** We compare pFedAFM with baselines under model-heterogeneous FL scenarios as follows.

<sup>1</sup><https://www.cs.toronto.edu/%7Ekriz/cifar.html>

**Table 2: Mean accuracy (%) in model-homogeneous FL.**

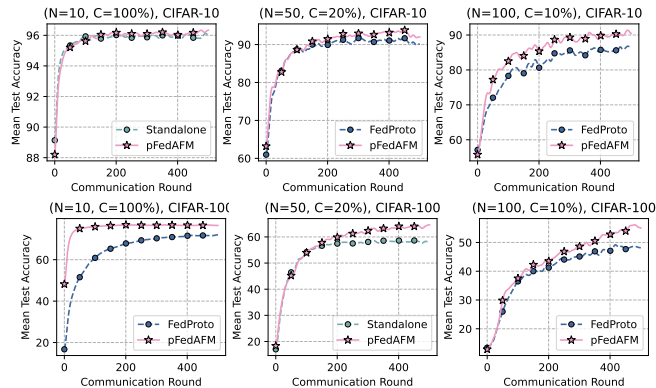
| FL Setting          | N=10, C=100% |              | N=50, C=20%  |              | N=100, C=10% |              |
|---------------------|--------------|--------------|--------------|--------------|--------------|--------------|
|                     | CIFAR-10     | CIFAR-100    | CIFAR-10     | CIFAR-100    | CIFAR-10     | CIFAR-100    |
| Standalone          | 96.35        | <b>74.32</b> | <b>95.25</b> | 62.38        | <b>92.58</b> | <b>54.93</b> |
| LG-FedAvg [23]      | <b>96.47</b> | 73.43        | 94.20        | 61.77        | 90.25        | 46.64        |
| FD [18]             | 96.30        | -            | -            | -            | -            | -            |
| FedProto [40]       | 95.83        | 72.79        | 95.10        | <b>62.55</b> | 91.19        | 54.01        |
| FML [38]            | 94.83        | 70.02        | 93.18        | 57.56        | 87.93        | 46.20        |
| FedKD [42]          | 94.77        | 70.04        | 92.93        | 57.56        | <b>90.23</b> | <b>50.99</b> |
| FedAPEN [33]        | <b>95.38</b> | <b>71.48</b> | <b>93.31</b> | <b>57.62</b> | 87.97        | 46.85        |
| <b>pFedAFM</b>      | <b>96.81</b> | <b>77.70</b> | <b>96.58</b> | <b>67.63</b> | <b>95.67</b> | <b>62.69</b> |
| pFedAFM-Best B.     | 0.34         | 3.38         | 1.33         | 5.08         | 3.09         | 7.76         |
| pFedAFM-Best S.C.B. | 1.43         | 6.22         | 3.27         | 10.01        | 5.44         | 11.70        |

Note: “-” denotes failure to converge. “**■**”: the best MHPFL method. “**□** Best B.” indicates the best baseline. “**□** Best S.C.B.” means the best same-category baseline.

**Table 3: Mean accuracy (%) in model-heterogeneous FL.**

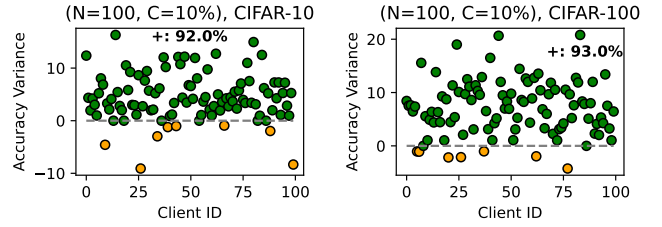
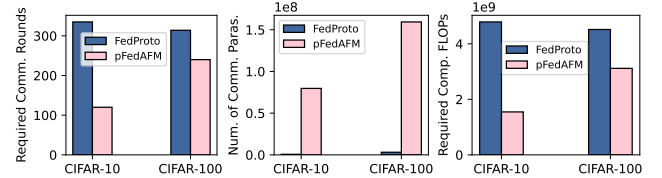
| FL Setting          | N=10, C=100% |              | N=50, C=20%  |              | N=100, C=10% |              |
|---------------------|--------------|--------------|--------------|--------------|--------------|--------------|
|                     | CIFAR-10     | CIFAR-100    | CIFAR-10     | CIFAR-100    | CIFAR-10     | CIFAR-100    |
| Standalone          | <b>96.53</b> | 72.53        | 95.14        | <b>62.71</b> | 91.97        | 53.04        |
| LG-FedAvg [23]      | 96.30        | 72.20        | 94.83        | 60.95        | 91.27        | 45.83        |
| FD [18]             | 96.21        | -            | -            | -            | -            | -            |
| FedProto [40]       | 96.51        | <b>72.59</b> | <b>95.48</b> | 62.69        | <b>92.49</b> | <b>53.67</b> |
| FML [38]            | 30.48        | 16.84        | -            | 21.96        | -            | 15.21        |
| FedKD [42]          | <b>80.20</b> | <b>53.23</b> | <b>77.37</b> | <b>44.27</b> | <b>73.21</b> | <b>37.21</b> |
| FedAPEN [33]        | -            | -            | -            | -            | -            | -            |
| <b>pFedAFM</b>      | <b>96.76</b> | <b>77.30</b> | <b>96.69</b> | <b>67.95</b> | <b>95.68</b> | <b>61.60</b> |
| pFedAFM-Best B.     | 0.23         | 4.71         | 1.21         | 5.24         | 3.19         | 7.93         |
| pFedAFM-Best S.C.B. | 16.56        | 24.07        | 19.32        | 23.68        | 22.47        | 24.39        |

Note: “-” denotes failure to converge. “**■**”: the best MHPFL method. “**□** Best B.” indicates the best baseline. “**□** Best S.C.B.” means the best same-category baseline.

**Figure 3: Average accuracy varies as rounds. Standalone or FedProto is the best baseline in each setting of Table 3.**

**Mean Accuracy.** Table 3 shows that pFedAFM obtains the highest mean accuracy across all FL settings. It achieves up to a 7.93% accuracy improvement over each FL setting’s best baseline, and up to 24.39% accuracy increment over each FL setting’s best same-category baseline. Significant accuracy improvements demonstrate that pFedAFM with a batch-level personalization based on dynamic dimension-level feature mixture adaptive to local data distribution enhances generalization and personalization of local models. Figure 3 shows that pFedAFM converges faster to higher accuracy. This reflects that pFedAFM with adaptive batch-level personalization promotes model convergence.

**Individual Accuracy.** Figure 4 depicts the individual accuracy variance of pFedAFM and the state-of-the-art baseline - FedProto

**Figure 4: Accuracy variance of individual clients.****Figure 5: Rounds, communication, and computation for target mean accuracy 90% on CIFAR-10 and 50% on CIFAR-100.**

under the most complicated FL setting ( $N = 100, C = 10\%$ ). It can be observed that 92% and 93% of the clients in pFedAFM performs better than those in FedProto on CIFAR-10 and CIFAR-100, respectively, verifying that pFedAFM with adaptive batch-level personalization enhances the personalization of local models.

**Communication Cost.** Under ( $N = 100, C = 10\%$ ), we measure the total communication costs of pFedAFM and FedProto reaching 90% and 50% target mean accuracy on CIFAR-10 and CIFAR-100, respectively. Figure 5(middle) shows that pFedAFM incurs a higher total communication cost than FedProto. Since pFedAFM exchanges homogeneous feature extractors while FedProto exchanges local seen-class average representations, pFedAFM incurs a higher one-round communication round, although Figure 5(left) shows that pFedAFM requires fewer rounds to reach the target mean accuracy. Nevertheless, compared with exchanging the complete local models under FedAvg, pFedAFM still incurs lower communication costs.

**Computational Overhead.** Figure 5(right) shows that pFedAFM incurs a lower computational cost than FedProto. FedProto has to compute the representations of each local sample after training and calculate each seen class’s average representation, while pFedAFM only needs to perform model training. Thus, pFedAFM incurs a lower per-round computational cost. Figure 5(left) shows that pFedAFM requires fewer rounds to achieve the target mean accuracy. Thus, it incurs a lower total computational overhead.

### 6.3 Case Studies

**6.3.1 Robustness to Pathological Non-IIDness.** We vary the number of seen classes for one client as  $\{2, 4, 6, 8, 10\}$  on CIFAR-10 and  $\{10, 30, 50, 70, 90, 100\}$  on CIFAR-100 under ( $N = 100, C = 10\%$ ). Figure 6 shows that pFedAFM always outperforms FedProto across all non-IIDness, indicating its robustness to non-IIDness. The model accuracy of the two algorithms degrades as the non-IIDness drops (the number of seen classes for one client increases). The more seen classes one client holds, the classification ability of the local

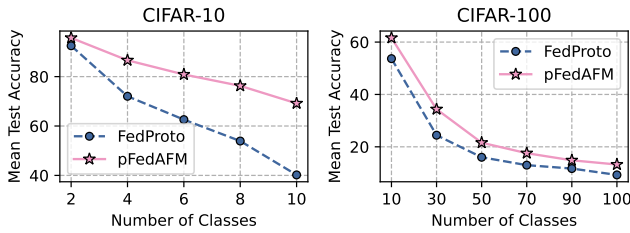


Figure 6: Robustness to pathological non-IIDness.

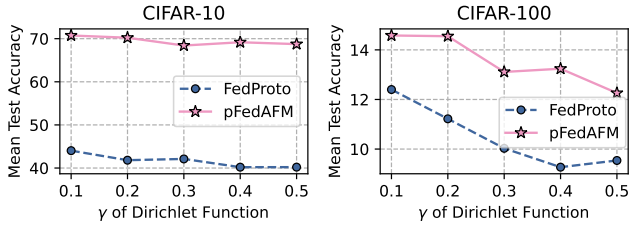


Figure 7: Robustness to practical non-IIDness.

model to each class drops (i.e., the local model’s generalization is enhanced, but personalization is weakened).

6.3.2 *Robustness to Practical Non-IIDness.* We vary the hyperparameter  $\gamma$  of the Dirichlet function as  $\{0.1, 0.2, 0.3, 0.4, 0.5\}$  on two datasets. Figure 7 shows that pFedAFM always performs higher accuracy than FedProto. Similar to the results under pathological non-IIDness, the model accuracy of the two methods also degrades as the non-IIDness drops ( $\gamma$  increases).

6.3.3 *Robustness to Learning Rate of Trainable Weight Vectors.* pFedAFM only introduces one hyperparameter - the learning rate  $\eta_\alpha$  of trainable weight vectors. We vary  $\eta_\alpha = \{0.001, 0.01, 0.1, 1\}$  on CIFAR-10 (non-IID:2/10) and CIFAR-100 (non-IID:10/100). For each setting, we use three random seeds for three trials. The results are displayed in Figure 8(left), the dots and shadows denote the average accuracy and its variance. It can be observed that pFedAFM’s accuracy rises as  $\eta_\alpha$  increases on CIFAR-10 and no obvious accuracy variations on CIFAR-100. Its accuracy under almost all  $\eta_\alpha$  settings outperform FedProto (92.49% on CIFAR-10, 53.67% on CIFAR-100), indicating its robustness to this hyperparameter.

## 6.4 Analysis of Trainable Weight Vectors

We randomly choose 2 clients under  $(N = 100, C = 10\%)$  on CIFAR-10 and CIFAR-100, respectively. We display the average of each client’s trainable weight vector for the local heterogeneous model varies as rounds. Figure 8(right) shows that different clients on the same dataset show diverse variations of the trainable weight vector’s average values, verifying that clients under pFedAFM train local personalized heterogeneous models adaptive to local data distributions. Besides, the average weights of the two clients are close to 0 and 0.5 on CIFAR-10 and CIFAR-100, respectively, reflecting that the generalized knowledge from the global homogeneous feature extractor and the personalized knowledge from the local heterogeneous model contributes differently to model performance in different training tasks. Therefore, it is necessary to utilize a pair

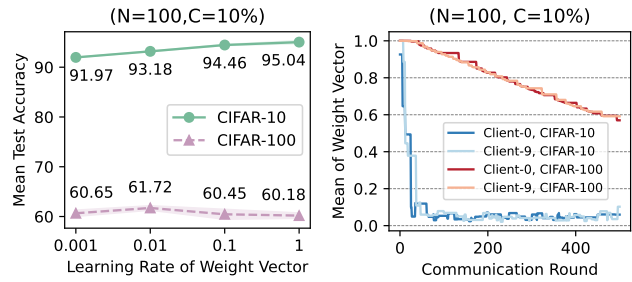


Figure 8: Left: robustness to the learning rate of the trainable weight vector  $\alpha$ . Right: Mean of the trainable weight vector  $\alpha$  varies as communication rounds.

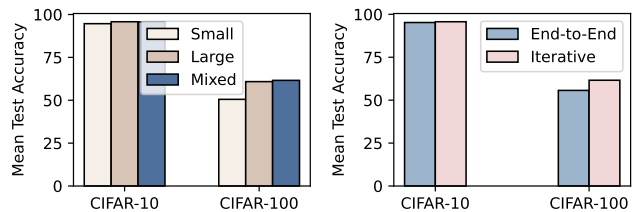


Figure 9: Left: mean test accuracy of global homogeneous small model, local heterogeneous large model, and the mixed model. Right: end-to-end training v.s. iterative training.

of trainable weight vectors to mix the generalized feature and the personalized feature based on local data distributions to balance between model generalization and personalization.

## 6.5 Ablation Study

6.5.1 *Small Model v.s. Large Model v.s. Mixed Model.* Section 6.4 shows that the average of the weight vector for the local heterogeneous model’s representations closes to 0 on CIFAR-10. We further verify the performance variation among the small model (the global homogeneous feature extractor and the local header), the large local heterogeneous model, and the mixed complete model under  $(N = 100, C = 10\%)$ . Figure 9(left) shows that the accuracy values of the three models are from low to high on both datasets, demonstrating the superiority of the mixed complete model. Although the weight vector’s average value of the local heterogeneous model is close to 0 on CIFAR-10, as shown in Figure 8(right), it still contributes to the performance of the mixed model.

6.5.2 *End-to-End Training v.s. Iterative Training.* An intuitive manner of training the global homogeneous feature extractor and the local heterogeneous model is updating them simultaneously in an end-to-end manner. It saves per-round training time compared with the proposed iterative training. Therefore, we study the accuracy achieved by these two approaches under  $(N = 100, C = 10\%)$ . Figure 9(right) shows that iterative training outperforms end-to-end training on both datasets, particularly on the more sophisticated CIFAR-100, verifying that pFedAFM improves model performance via effective bi-directional knowledge transfer.



## 7 DISCUSSION

In this section, we discuss the privacy, communication and computational costs of the proposed pFedAFM as follows.

**Privacy.** Under pFedAFM, only the small homogeneous feature extractors are transmitted between clients and the server. The local data and heterogeneous models are never exposed. Thus, data and model privacy is preserved.

**Communication Costs.** Clients and the server exchange the small homogeneous feature extractors which are much smaller than the local heterogeneous models. The communication costs are lower than exchanging the local heterogeneous models.

**Computational Costs.** Besides training the local heterogeneous models, clients also train the weight vectors and the small homogeneous feature extractors. Although the computational cost in one round is higher, the total computational costs also depend on the rounds required for convergence. The adaptive batch-level personalization improves convergence rates. Thus, the overall computational costs are acceptable.

## 8 CONCLUSIONS

This paper proposed an effective and efficient MHPFL algorithm, pFedAFM, capable of handling batch-level data heterogeneity. It fuses the knowledge of local heterogeneous models by sharing an additional homogeneous small feature extractor across clients. Iterative training effectively facilitates the bidirectional transfer of global generalized knowledge and local personalized knowledge, enhancing the generalization and personalization of local models. The trainable weight vectors dynamically balance the generalization and personalization by mixing generalized features and personalized features adaptive to local data distribution variations across different batches. Theoretical analysis proves it can converge over time with a  $\mathcal{O}(1/T)$  convergence rate. Experiments demonstrate that it obtains the state-of-the-art model performance with low communication and computational costs.

## REFERENCES

- [1] Jin-Hyun Ahn et al. 2019. Wireless Federated Distillation for Distributed Edge Learning with Heterogeneous Data. In *Proc. PIMRC*. IEEE, Istanbul, Turkey, 1–6.
- [2] Jin-Hyun Ahn et al. 2020. Cooperative Learning VIA Federated Distillation OVER Fading Channels. In *Proc. ICASSP*. IEEE, Barcelona, Spain, 8856–8860.
- [3] Samiul Alam et al. 2022. FedRolex: Model-Heterogeneous Federated Learning with Rolling Sub-Model Extraction. In *Proc. NeurIPS*. , virtual.
- [4] Sara Babakniya et al. 2023. Revisiting Sparsity Hunting in Federated Learning: Why does Sparsity Consensus Matter? *Transactions on Machine Learning Research* 1, 1 (2023), 1.
- [5] Yun-Hin Chan, Rui Zhou, Running Zhao, Zhihan JIANG, and Edith C. H. Ngai. 2024. Internal Cross-layer Gradients for Extending Homogeneity to Heterogeneity in Federated Learning. In *Proc. ICLR*. OpenReview.net, Vienna, Austria, 1.
- [6] Hongyan Chang et al. 2021. Cronus: Robust and Heterogeneous Collaborative Learning with Black-Box Knowledge Transfer. In *Proc. NeurIPS Workshop*. , virtual.
- [7] Jiangui Chen et al. 2021. FedMatch: Federated Learning Over Heterogeneous Question Answering Data. In *Proc. CIKM*. ACM, virtual, 181–190.
- [8] Sijie Cheng et al. 2021. FedGEMS: Federated Learning of Larger Server Models via Selective Knowledge Fusion. *CoRR abs/2110.11027* (2021).
- [9] Yae Jee Cho et al. 2022. Heterogeneous Ensemble Knowledge Transfer for Training Large Models in Federated Learning. In *Proc. IJCAI*. ijcai.org, virtual, 2881–2887.
- [10] Liam Collins et al. 2021. Exploiting Shared Representations for Personalized Federated Learning. In *Proc. ICML*, Vol. 139. PMLR, virtual, 2089–2099.
- [11] Enmao Diao. 2021. HeteroFL: Computation and Communication Efficient Federated Learning for Heterogeneous Clients. In *Proc. ICLR*. OpenReview.net, Virtual Event, Austria, 1.
- [12] Chaoyang He et al. 2020. Group Knowledge Transfer: Federated Learning of Large CNNs at the Edge. In *Proc. NeurIPS*. , virtual.
- [13] S. Horváth. 2021. FJORD: Fair and Accurate Federated Learning under heterogeneous targets with Ordered Dropout. In *Proc. NIPS*. OpenReview.net, Virtual, 12876–12889.
- [14] Wenke Huang et al. 2022. Few-Shot Model Agnostic Federated Learning. In *Proc. MM*. ACM, Lisboa, Portugal, 7309–7316.
- [15] Wenke Huang et al. 2022. Learn from Others and Be Yourself in Heterogeneous Federated Learning. In *Proc. CVPR*. IEEE, virtual, 10133–10143.
- [16] Sohei Itahara et al. 2023. Distillation-Based Semi-Supervised Federated Learning for Communication-Efficient Collaborative Training With Non-IID Private Data. *IEEE Trans. Mob. Comput.* 22, 1 (2023), 191–205.
- [17] Jaehye Jang et al. 2022. FedClassAvg: Local Representation Learning for Personalized Federated Learning on Heterogeneous Neural Networks. In *Proc. ICPP*. ACM, virtual, 76:1–76:10.
- [18] Eunjeong Jeong et al. 2018. Communication-Efficient On-Device Machine Learning: Federated Distillation and Augmentation under Non-IID Private Data. In *Proc. NeurIPS Workshop on Machine Learning on the Phone and other Consumer Devices*. , virtual.
- [19] Peter Kairouz et al. 2021. Advances and Open Problems in Federated Learning. *Foundations and Trends in Machine Learning* 14, 1–2 (2021), 1–210.
- [20] Alex Krizhevsky et al. 2009. *Learning multiple layers of features from tiny images*. Toronto, ON, Canada, .
- [21] Daliang Li and Junpu Wang. 2019. FedMD: Heterogeneous Federated Learning via Model Distillation. In *Proc. NeurIPS Workshop*. , virtual.
- [22] Qimbin Li et al. 2021. Practical One-Shot Federated Learning for Cross-Silo Setting. In *Proc. IJCAI*. ijcai.org, virtual, 1484–1490.
- [23] Paul Pu Liang et al. 2020. Think locally, act globally: Federated learning with local and global representations. *arXiv preprint arXiv:2001.01523* 1, 1 (2020).
- [24] Tao Lin et al. 2020. Ensemble Distillation for Robust Model Fusion in Federated Learning. In *Proc. NeurIPS*. , virtual.
- [25] Chang Liu et al. 2022. Completely Heterogeneous Federated Learning. *CoRR abs/2210.15865* (2022).
- [26] Xiaofeng Lu et al. 2022. Heterogeneous Model Fusion Federated Learning Mechanism Based on Model Mapping. *IEEE Internet Things J.* 9, 8 (2022), 6058–6068.
- [27] Disha Makhija et al. 2022. Architecture Agnostic Federated Learning for Neural Networks. In *Proc. ICML*, Vol. 162. PMLR, virtual, 14860–14870.
- [28] Brendan McMahan et al. 2017. Communication-Efficient Learning of Deep Networks from Decentralized Data. In *Proc. AISTATS*, Vol. 54. PMLR, Fort Lauderdale, FL, USA, 1273–1282.
- [29] Duy Phuong Nguyen et al. 2023. Enhancing Heterogeneous Federated Learning with Knowledge Extraction and Multi-Model Fusion. In *Proc. SC Workshop*. ACM, Denver, CO, USA, 36–43.
- [30] Jaehoon Oh et al. 2022. FedBABU: Toward Enhanced Representation for Federated Image Classification. In *Proc. ICLR*. OpenReview.net, virtual.
- [31] Sejun Park et al. 2023. Towards Understanding Ensemble Distillation in Federated Learning. In *Proc. ICML*, Vol. 202. PMLR, Honolulu, Hawaii, USA, 27132–27187.
- [32] Krishna Pillutla et al. 2022. Federated Learning with Partial Model Personalization. In *Proc. ICML*, Vol. 162. PMLR, virtual, 17716–17758.
- [33] Zhen Qin et al. 2023. FedAPEN: Personalized Cross-silo Federated Learning with Adaptability to Statistical Heterogeneity. In *Proc. KDD*. ACM, Long Beach, CA, USA, 1954–1964.
- [34] Sebastian Ruder. 2016. An overview of gradient descent optimization algorithms. *CoRR abs/1609.04747* (2016), 1.
- [35] Felix Sattler et al. 2021. FEDAUx: Leveraging Unlabeled Auxiliary Data in Federated Learning. *IEEE Trans. Neural Networks Learn. Syst.* 1, 1 (2021), 1–13.
- [36] Felix Sattler et al. 2022. CFD: Communication-Efficient Federated Distillation via Soft-Label Quantization and Delta Coding. *IEEE Trans. Netw. Sci. Eng.* 9, 4 (2022), 2025–2038.
- [37] Aviv Shamsian et al. 2021. Personalized Federated Learning using Hypernetworks. In *Proc. ICML*, Vol. 139. PMLR, virtual, 9489–9502.
- [38] Tao Shen et al. 2020. Federated Mutual Learning. *CoRR abs/2006.16765* (2020).
- [39] Xiaorong Shi, Liping Yi, Xiaoguang Liu, and Gang Wang. 2023. FFEDCL: Fair Federated Learning with Contrastive Learning. In *Proc. ICASSP, Rhodes Island, Greece*. IEEE, 1–5.
- [40] Yue Tan et al. 2022. FedProto: Federated Prototype Learning across Heterogeneous Clients. In *Proc. AAAI*. AAAI Press, virtual, 8432–8440.
- [41] Jiaqi Wang et al. 2023. Towards Personalized Federated Learning via Heterogeneous Model Reassembly. In *Proc. NeurIPS*. OpenReview.net, New Orleans, Louisiana, USA, 13.
- [42] Chuhan Wu et al. 2022. Communication-efficient federated learning via knowledge distillation. *Nature Communications* 13, 1 (2022), 2032.
- [43] Liping Yi, Xiaorong Shi, Nan Wang, Gang Wang, Xiaoguang Liu, Zhuan Shi, and Han Yu. 2024. pFedKT: Personalized federated learning with dual knowledge transfer. *Knowledge-Based Systems* 292 (2024), 111633.
- [44] Liping Yi, Xiaorong Shi, Nan Wang, Ziyue Xu, Gang Wang, and Xiaoguang Liu. 2023. pFedLHNs: Personalized Federated Learning via Local Hypernetworks. In *Proc. ICANN*, Vol. 1. Springer, 516–528.

- [45] Liping Yi, Xiaorong Shi, Nan Wang, Jinsong Zhang, Gang Wang, and Xiaoguang Liu. 2024. FedPE: Adaptive Model Pruning-Expanding for Federated Learning on Mobile Devices. *IEEE Transactions on Mobile Computing* (2024), 1–18.
- [46] Liping Yi, Xiaorong Shi, Wenrui Wang, Gang Wang, and Xiaoguang Liu. 2023. FedRRA: Reputation-Aware Robust Federated Learning against Poisoning Attacks. In *Proc. IJCNN*. IEEE, 1–8.
- [47] Liping Yi, Gang Wang, and Xiaoguang Liu. 2022. QSFL: A Two-Level Uplink Communication Optimization Framework for Federated Learning. In *Proc. ICML*, Vol. 162. PMLR, 25501–25513.
- [48] Liping Yi, Gang Wang, Xiaoguang Liu, Zhuan Shi, and Han Yu. 2023. FedGH: Heterogeneous Federated Learning with Generalized Global Header. In *Proc. MM, Ottawa, ON, Canada*. ACM, 8686–8696.
- [49] Liping Yi, Han Yu, Chao Ren, Heng Zhang, Gang Wang, Xiaoguang Liu, and Xiaoxiao Li. 2024. pFedMoE: Data-Level Personalization with Mixture of Experts for Model-Heterogeneous Personalized Federated Learning. *CoRR abs/2402.01350* (2024).
- [50] Liping Yi, Han Yu, Zhuan Shi, Gang Wang, Xiaoguang Liu, Lizhen Cui, and Xiaoxiao Li. 2024. FedSSA: Semantic Similarity-based Aggregation for Efficient Model-Heterogeneous Personalized Federated Learning. In *IJCAI*.
- [51] Liping Yi, Han Yu, Gang Wang, and Xiaoguang Liu. 2023. FedLoRA: Model-Heterogeneous Personalized Federated Learning with LoRA Tuning. *CoRR abs/2310.13283* (2023).
- [52] Liping Yi, Han Yu, Gang Wang, and Xiaoguang Liu. 2023. pFedES: Model Heterogeneous Personalized Federated Learning with Feature Extractor Sharing. *CoRR abs/2311.06879* (2023).
- [53] Liping Yi, Jinsong Zhang, Rui Zhang, Jiaqi Shi, Gang Wang, and Xiaoguang Liu. 2020. SU-Net: An Efficient Encoder-Decoder Model of Federated Learning for Brain Tumor Segmentation. In *Proc. ICANN*, Vol. 12396. Springer, 761–773.
- [54] Fuxun Yu et al. 2021. Fed2: Feature-Aligned Federated Learning. In *Proc. KDD*. ACM, virtual, 2066–2074.
- [55] Sixing Yu et al. 2022. Resource-aware Federated Learning using Knowledge Extraction and Multi-model Fusion. *CoRR abs/2208.07978* (2022).
- [56] Jie Zhang et al. 2021. Parameterized Knowledge Transfer for Personalized Federated Learning. In *Proc. NeurIPS*. OpenReview.net, virtual, 10092–10104.
- [57] Jie Zhang et al. 2023. Towards Data-Independent Knowledge Transfer in Model-Heterogeneous Federated Learning. *IEEE Trans. Computers* 72, 10 (2023), 2888–2901.
- [58] Lan Zhang et al. 2022. FedZKT: Zero-Shot Knowledge Transfer towards Resource-Constrained Federated Learning with Heterogeneous On-Device Models. In *Proc. ICDCS*. IEEE, virtual, 928–938.
- [59] Zhilu Zhang and Mert R. Sabuncu. 2018. Generalized Cross Entropy Loss for Training Deep Neural Networks with Noisy Labels. In *Proc. NeurIPS*. Curran Associates Inc., Montréal, Canada, 8792–8802.
- [60] Hangyu Zhu et al. 2021. Federated learning on non-IID data: A survey. *Neurocomputing* 465 (2021), 371–390.
- [61] Zhuangdi Zhu et al. 2021. Data-Free Knowledge Distillation for Heterogeneous Federated Learning. In *Proc. ICML*, Vol. 139. PMLR, virtual, 12878–12889.
- [62] Zhuangdi Zhu et al. 2022. Resilient and Communication Efficient Learning for Heterogeneous Federated Systems. In *Proc. ICML*, Vol. 162. PMLR, virtual, 27504–27526.

## A THEORETICAL PROOFS

### A.1 Proof for Lemma 1

An arbitrary client  $k$ 's local mixed complete model  $h$  can be updated by  $h_{t+1} = h_t - \eta g_{h,t}$  in the  $(t+1)$ -th round, and following Assumption 1, we can obtain

$$\begin{aligned} \mathcal{L}_{tE+1} &\leq \mathcal{L}_{tE+0} + \langle \nabla \mathcal{L}_{tE+0}, (h_{tE+1} - h_{tE+0}) \rangle + \frac{L_1}{2} \|h_{tE+1} - h_{tE+0}\|_2^2 \\ &= \mathcal{L}_{tE+0} - \eta \langle \nabla \mathcal{L}_{tE+0}, g_{h,tE+0} \rangle + \frac{L_1 \eta^2}{2} \|g_{h,tE+0}\|_2^2. \end{aligned} \quad (22)$$

Taking the expectation of both sides of the inequality concerning the random variable  $\xi_{tE+0}$ , we obtain

$$\begin{aligned} \mathbb{E}[\mathcal{L}_{tE+1}] &\leq \mathcal{L}_{tE+0} - \eta \mathbb{E}[\langle \nabla \mathcal{L}_{tE+0}, g_{h,tE+0} \rangle] + \frac{L_1 \eta^2}{2} \mathbb{E}[\|g_{h,tE+0}\|_2^2] \\ &\stackrel{(a)}{=} \mathcal{L}_{tE+0} - \eta \|\nabla \mathcal{L}_{tE+0}\|_2^2 + \frac{L_1 \eta^2}{2} \mathbb{E}[\|g_{h,tE+0}\|_2^2] \\ &\stackrel{(b)}{\leq} \mathcal{L}_{tE+0} - \eta \|\nabla \mathcal{L}_{tE+0}\|_2^2 + \frac{L_1 \eta^2}{2} (\mathbb{E}[\|g_{h,tE+0}\|_2^2] + \text{Var}(g_{h,tE+0})) \\ &\stackrel{(c)}{=} \mathcal{L}_{tE+0} - \eta \|\nabla \mathcal{L}_{tE+0}\|_2^2 + \frac{L_1 \eta^2}{2} (\|\nabla \mathcal{L}_{tE+0}\|_2^2 + \text{Var}(g_{h,tE+0})) \\ &\stackrel{(d)}{\leq} \mathcal{L}_{tE+0} - \eta \|\nabla \mathcal{L}_{tE+0}\|_2^2 + \frac{L_1 \eta^2}{2} (\|\nabla \mathcal{L}_{tE+0}\|_2^2 + \sigma^2) \\ &= \mathcal{L}_{tE+0} + \left(\frac{L_1 \eta^2}{2} - \eta\right) \|\nabla \mathcal{L}_{tE+0}\|_2^2 + \frac{L_1 \eta^2 \sigma^2}{2}. \end{aligned} \quad (23)$$

(a), (c), (d) follow Assumption 2 and (b) follows  $\text{Var}(x) = \mathbb{E}[x^2] - (\mathbb{E}[x])^2$ .

Taking the expectation of both sides of the inequality for the model  $h$  over  $E$  iterations, we obtain

$$\mathbb{E}[\mathcal{L}_{tE+1}] \leq \mathcal{L}_{tE+0} + \left(\frac{L_1 \eta^2}{2} - \eta\right) \sum_{e=1}^E \|\nabla \mathcal{L}_{tE+e}\|_2^2 + \frac{L_1 E \eta^2 \sigma^2}{2}. \quad (24)$$

### A.2 Proof for Lemma 2

$$\begin{aligned} \mathcal{L}_{(t+1)E+0} &= \mathcal{L}_{(t+1)E} + \mathcal{L}_{(t+1)E+0} - \mathcal{L}_{(t+1)E} \\ &\stackrel{(a)}{\approx} \mathcal{L}_{(t+1)E} + \eta \|\theta_{(t+1)E+0} - \theta_{(t+1)E}\|_2^2 \\ &\stackrel{(b)}{\leq} \mathcal{L}_{(t+1)E} + \eta \delta^2. \end{aligned} \quad (25)$$

(a): we can use the gradient of parameter variations to approximate the loss variations, *i.e.*,  $\Delta \mathcal{L} \approx \eta \cdot \|\Delta \theta\|_2^2$ . (b) follows Assumption 3.

Taking the expectation of both sides of the inequality to the random variable  $\xi$ , we obtain

$$\mathbb{E}[\mathcal{L}_{(t+1)E+0}] \leq \mathbb{E}[\mathcal{L}_{tE+1}] + \eta \delta^2. \quad (26)$$

### A.3 Proof for Theorem 1

Substituting Lemma 1 into the right side of Lemma 2's inequality, we obtain

$$\mathbb{E}[\mathcal{L}_{(t+1)E+0}] \leq \mathcal{L}_{tE+0} + \left(\frac{L_1 \eta^2}{2} - \eta\right) \sum_{e=0}^E \|\nabla \mathcal{L}_{tE+e}\|_2^2 + \frac{L_1 E \eta^2 \sigma^2}{2} + \eta \delta^2. \quad (27)$$

### A.4 Proof for Theorem 2

Interchanging the left and right sides of Eq. (27), we obtain

$$\sum_{e=0}^E \|\nabla \mathcal{L}_{tE+e}\|_2^2 \leq \frac{\mathcal{L}_{tE+0} - \mathbb{E}[\mathcal{L}_{(t+1)E+0}] + \frac{L_1 E \eta^2 \sigma^2}{2} + \eta \delta^2}{\eta - \frac{L_1 \eta^2}{2}}. \quad (28)$$

Taking the expectation of both sides of the inequality over rounds  $t = [0, T-1]$  to  $W$ , we obtain

$$\frac{1}{T} \sum_{t=0}^{T-1} \sum_{e=0}^{E-1} \|\nabla \mathcal{L}_{tE+e}\|_2^2 \leq \frac{\frac{1}{T} \sum_{t=0}^{T-1} [\mathcal{L}_{tE+0} - \mathbb{E}[\mathcal{L}_{(t+1)E+0}]] + \frac{L_1 E \eta^2 \sigma^2}{2} + \eta \delta^2}{\eta - \frac{L_1 \eta^2}{2}}. \quad (29)$$

Let  $\Delta = \mathcal{L}_{t=0} - \mathcal{L}^* > 0$ , then  $\sum_{t=0}^{T-1} [\mathcal{L}_{tE+0} - \mathbb{E}[\mathcal{L}_{(t+1)E+0}]] \leq \Delta$ , we can get

$$\frac{1}{T} \sum_{t=0}^{T-1} \sum_{e=0}^{E-1} \|\nabla \mathcal{L}_{tE+e}\|_2^2 \leq \frac{\frac{\Delta}{T} + \frac{L_1 E \eta^2 \sigma^2}{2} + \eta \delta^2}{\eta - \frac{L_1 \eta^2}{2}}. \quad (30)$$

If the above equation converges to a constant  $\epsilon$ , *i.e.*,

$$\frac{\frac{\Delta}{T} + \frac{L_1 E \eta^2 \sigma^2}{2} + \eta \delta^2}{\eta - \frac{L_1 \eta^2}{2}} < \epsilon, \quad (31)$$

then

$$T > \frac{\Delta}{\epsilon(\eta - \frac{L_1 \eta^2}{2}) - \frac{L_1 E \eta^2 \sigma^2}{2} - \eta \delta^2}. \quad (32)$$

Since  $T > 0$ ,  $\Delta > 0$ , we can get

$$\epsilon(\eta - \frac{L_1 \eta^2}{2}) - \frac{L_1 E \eta^2 \sigma^2}{2} - \eta \delta^2 > 0. \quad (33)$$

Solving the above inequality yields

$$\eta < \frac{2(\epsilon - \delta^2)}{L_1(\epsilon + E\sigma^2)}. \quad (34)$$

Since  $\epsilon$ ,  $L_1$ ,  $\sigma^2$ ,  $\delta^2$  are all constants greater than 0,  $\eta$  has solutions. Therefore, when the learning rate  $\eta$  satisfies the above condition, any client's local mixed complete heterogeneous model can converge. Notice that the learning rate of the local complete heterogeneous model involves  $\{\eta_\theta, \eta_\omega, \eta_\alpha\}$ , so it's crucial to set reasonable them to ensure model convergence. Since all terms on the right side of Eq. (30) except for  $1/T$  are constants, hence pFedAFM's non-convex convergence rate is  $\epsilon \sim \mathcal{O}(1/T)$ .